شـــكل التـــوزيع المعمم فريشـــت والتغير في معـــدل الفشل (خصائص وتطبيقات) .

فاطمة سعيد علـي الـزّوق ـ كلّيـة الآداب بالجميل ـ جامعة صبراتة

الملخّـــص :

تمت دراســـة نموذج جديد مكوّن من خمس معلمات يسمى توزيع معدل الفشل الخطي المعمم (GLFRF). يوفّـــر توزيــــع Fréchet GLFRF أشكالًا لمعدلات الفشـــل مرتبة وغير مرتبة بما في ذلك شكل حوض الاستحمام وشكل وحوض الاستحمام المعدل والأشكال أحادية النســـق الشائعة جدًا في المجالات التطبيقية. ويتم اشتقاق بعض الخصائص الرياضية لنموذج GLFRF الدّالـــة الكميـــة، واللحظات العادية وغير المكتملة، وإحصاءات الترتيب، ووظيفة التوليـــد، ولحظات الأعمار المتبقية والمعكوسة. ويمكن التعبير عن دالة الكثافة لتـــوزيع GLFRF كمجموعة خطية من Fréchet، وتـــم اعتماد دالة الاحتمالية القصوى لتقدير معلمات GLFRF. تم إثبات مرونة التوزيع الجديد بشـــكل تجريبي باستخدام مجموعتين من مجموعات البيانات الواقعية. يوفر توزيــــع GLFRF ملاءمة أفضل للمقارنةً بتوزيعات Kumaraswamy-Fréchet، و Kumaraswamy Marshall، و Olkin Fréchet، و beta-Fréchet، و exponentiated fréchet، و gamma الممتدةFréchet.

The Generalized Fréchet Distribution with Variable Hazard Rate Shapes: Properties and Applications

Fatimah Saeid Ali Alzawq

ABSTRACT

A new five-parameter model called the generalized linear failure rate Fréchet (GLFRF) distribution is studied. The GLFRF distribution provides monotone and nonmonotone hazard rate shapes including bathtub, modified bathtub and unimodal shapes which are very common in applied fields. Some mathematical properties of the GLFRF model such as quantile function, ordinary and incomplete moments, order statistics, generating function, moments of residual and reversed resedual lifes are derived. The density

function of the GLFRF distribution can be expressed as a linear combination of Fréchet densities. The maximum likelihood approach is adopted to estimate the GLFRF parameters. The flexibility of the new distribution is proved empirically using two real-life data sets. The GLFRF distribution provides better fit as compared to the Kumaraswamy–Fréchet, Kumaraswamy Marshall–Olkin Fréchet, beta-Fréchet, exponentiated-Fréchet, and gamma extended-Fréchet distributions.

KEYWORDS

Fréchet distribution, GLFR-G family, order statistic, generating function, maximum likelihood.

1. Introduction

The Fréchet distribution (Maurice Fréchet, 1924)) is an important distribution which has wide applicability in the extreme value theory. The Fréchet distribution has some applications in air pollution, rainfall, and floods (Kotz and Nadarajah, 2000), engineering applications (Harlow, 2002), modeling wind speed data (Zaharim et al., 2009), and advanced mathematical results on regularly varying (Resnick, 2013), among others. More details about the applications of Fréchet distribution can be found in Kotz and Nadarajah (2000).

The statistical literature contains several generalized modified extensions of the Fréchet distribution icluding the exponentiated–Fréchet (Nadarajah and Kotz, 2003), beta–Fréchet (Nadarajah and Gupta, 2004), transmuted–Fréchet (Mahmoud and Mandouh, 2013), Marshall-Olkin Fréchet (Krishna et al., 2013), gamma extended Fréchet (Silva et al., 2013), Kumaraswamy–Fréchet (Mead and Abd-Eltawab, 2014), transmuted exponentiated–Fréchet (Elbatal et al., 2014), transmuted Marshall–Olkin Fréchet (Afify et al., 2015), Kumaraswamy Marshall-Olkin Fréchet (Afify et al., 2016), Weibull–Fréchet (Afify et al., 2016b), modified–Fréchet (Tablada and Cordeiro, 2017), beta exponential–Fréchet (Mead et al., 2017), odd Lindley–Fréchet (Mansour et al., 2018), Burr–X Fréchet (Abouelmagd, et al., 2018), modified Kies–Fréchet (Al Sobhi, 2021), logarithmic-transformed Fréchet (Afify et al., 2021), and extended Weibull– Fréchet (Hussein et al., 2022), among many others.

In this paper, we propose a new flexible five-parameter Fréchet distribution called the generalized linear failure rate Fréchet (GLFRF) distribution and study some of its mathematical properties. We address the applicability of the GLFRF model by analyzing two real-life data applications. The new GLFRF distribution is generated by applying the generalized linear failure rate-G (GLFR-G) family (Afify et al., 2022) to the Fréchet distribution.

The proposed GLFRF distribution is very flexible and has some desirable properties as follows: (i) The GLFRF density can be right skewed, symmetrical, reversed-J shaped, left skewed, unimodal, and concave down; (ii) The GLFRF hazard rate function (HRF) can be increasing, unimodal, decreasing, bathtub, J-shape reversed-J shape, and modified bathtub; (iii) It can be used to model several real-life data from applied fields. The GLFRF model provides better fit as compared to other competing Fréchet distributions.

The rest of this paper is outlined as follows. The GLFR-G family is presented in Section 2. Section 3 is devoted to introducing the GLFRF distribution, providing its special cases and some plots for its PDF and HRF. The mixture representation for the GLFRF density is given in Section 4. The key properties of the GLFRF model are derived in Section 5. The GLFRF parameters are estimated via the maximum likelihood in Section 6. Section 7 provides numerical simulations for exploring the behavior of the estimates. Two real-life data applications are addressed in Section 8. Some concluding remarks are offered in Section 9.

2. The GLFR-G Family

In this section, we provide some details about the GLFR-G family introduced by Afify et al. (2022). The cumulative distribution function (CDF) of the GLFR-G family reduces (for $x \in \mathbb{R}$)

$$F(x; \boldsymbol{\psi}) = \left(1 - \exp\left\{-\lambda\left[\frac{G(x;\boldsymbol{\varphi})}{1-G(x;\boldsymbol{\varphi})}\right] - \frac{\phi}{2}\left[\frac{G(x;\boldsymbol{\varphi})}{1-G(x;\boldsymbol{\varphi})}\right]^2\right\}\right)^\gamma,$$

(1)

where $\boldsymbol{\psi} = (\lambda, \phi, \gamma, \boldsymbol{\varphi}^T)^T$, $\lambda > 0$ and $\phi > 0$ are scale parameters, and $\gamma > 0$ is a shape parameter. The corresponding pdf is

$$f(x;\boldsymbol{\psi}) = \frac{g(x;\boldsymbol{\varphi})[\lambda\,\gamma + \gamma(\phi-\lambda)G(x;\boldsymbol{\varphi})]}{[1-G(x;\boldsymbol{\varphi})]^3}\exp\left\{-\lambda\left[\frac{G(x;\boldsymbol{\varphi})}{1-G(x;\boldsymbol{\varphi})}\right]\right.$$
$$\left.-\frac{\phi}{2}\left[\frac{G(x;\boldsymbol{\varphi})}{1-G(x;\boldsymbol{\varphi})}\right]^2\right\}$$
$$\times\left(1-\exp\left\{-\lambda\left[\frac{G(x;\varphi)}{1-G(x;\varphi)}\right]-\frac{\phi}{2}\left[\frac{G(x;\varphi)}{1-G(x;\varphi)}\right]^2\right\}\right)^{\gamma-1}.$$

(2)

The HRF and reverse HRF (RHRF) of the GLFR-G family are given by

$$h(x;\boldsymbol{\psi}) = \frac{\frac{g(x;\varphi)[\lambda\gamma+\gamma(\phi-\lambda)G(x;\varphi)]}{[1-G(x;\varphi)]^3}\exp\left\{-\lambda\left[\frac{G(x;\varphi)}{1-G(x;\varphi)}\right]-\frac{\phi}{2}\left[\frac{G(x;\varphi)}{1-G(x;\varphi)}\right]^2\right\}}{\left(1-\exp\left\{-\lambda\left[\frac{G(x;\varphi)}{1-G(x;\varphi)}\right]-\frac{\phi}{2}\left[\frac{G(x;\varphi)}{1-G(x;\varphi)}\right]^2\right\}\right)^{1-\theta}-\left(1-\exp\left\{-\lambda\left[\frac{G(x;\varphi)}{1-G(x;\varphi)}\right]-\frac{\phi}{2}\left[\frac{G(x;\varphi)}{1-G(x;\varphi)}\right]^2\right\}\right)}$$

(3)

and

$$\tau(x;\boldsymbol{\psi}) = \frac{\lambda\,\gamma g(x;\varphi)+\gamma(\phi-\lambda)g(x;\varphi)G(x;\varphi)}{[1-G(x;\varphi)]^3\left(\exp\left\{\lambda\left[\frac{G(x;\varphi)}{1-G(x;\varphi)}\right]+\frac{\phi}{2}\left[\frac{G(x;\varphi)}{1-G(x;\varphi)}\right]^2\right\}-1\right)}.$$

(4)

The cumulative HRF (CHRF) of the GLFR-G family takes the form

$$H(x;\boldsymbol{\varphi}) = -\log\left[1-\left(1-\exp\left\{-\lambda\left[\frac{G(x;\boldsymbol{\varphi})}{1-G(x;\boldsymbol{\varphi})}\right]-\frac{\phi}{2}\left[\frac{G(x;\boldsymbol{\varphi})}{1-G(x;\boldsymbol{\varphi})}\right]^2\right\}\right)^{\gamma}\right].$$

(5)

The GLFR-G family has some special sub-families (Afify et al., 2022) which are reported in Table 1 for selected parametric values.

Table 1: Special sub-families of the GLFR-G family

λ	ϕ	γ	Sub-family	Authors
-	-	1	Linear failure rate-G (LFR-G)	New
0	-	-	Generalized Rayleigh-G (GR-G)	New
0	-	1	Rayleigh-G (R-G)	Bourguignon et al. (2014)
-	0	1	Exponential-G (E-G)	Bourguignon et al. (2014)
-	0	-	Odd generalized exponential-G (OGE-G)	Tahir et al. (2015)

3. The GLFRF Distribution

In this section, we define the GLFRF distribution which is generated by applying the GLFR-G family by choosing the Fréchet distribution as a baseline model.

The CDF and PDF of the Fréchet distribution take the forms

$$G(x; \delta, \eta) = e^{-\left(\frac{\delta}{x}\right)^{\eta}}, \ x > 0 \tag{6}$$

and

$$g(x; \delta, \eta) = \eta \delta^{\eta} x^{-\eta-1} e^{-\left(\frac{\delta}{x}\right)^{\eta}}, \ x > 0, \tag{7}$$

where $\delta > 0$ is a scale parameter and $\eta > 0$ is a shape parameter.

The nth ordinary and incomplete moments of $X \sim$ Fréchet(δ, η) are given (for $n < \eta$) by

$$\mu'_n = \delta^n \ \Gamma\left(1 - \frac{n}{\eta}\right) \quad \text{and} \quad \varphi_n(t) = \delta^n \ \gamma(1 - n/\eta, (\delta/t)^{\eta}),$$

where $\Gamma(s) = \int_0^{\infty} z^{s-1} e^{-z} dz$ is the complete gamma function (GF) and $\gamma(s, k) = \int_0^k z^{s-1} e^{-z} dz$ is the lower incomplete GF.

Hence, the CDF of the new GLFRF distribution follows, by inserting the CDF (6) of the Fréchet distribution in Equation (1), as

$$F(x; \boldsymbol{\psi}) = \left(1 - \exp\left\{-\lambda\left[e^{\left(\frac{\delta}{x}\right)^{\eta}} - 1\right]^{-1} - \frac{\phi}{2}\left[e^{\left(\frac{\delta}{x}\right)^{\eta}} - 1\right]^{-2}\right\}\right)^{\gamma}, \ x > 0,$$

(8)

where $\boldsymbol{\psi} = (\lambda, \phi, \gamma, \delta, \eta)^T$, $\lambda > 0$, $\phi > 0$ and $\delta > 0$ are scale parameters, and $\gamma > 0$, and $\eta > 0$ are shape parameters.

The PDF of the GLFRF model has the form

$$f(x; \boldsymbol{\psi}) = \frac{\eta \delta^{\eta} x^{-\eta-1} e^{-\left(\frac{\delta}{x}\right)^{\eta}} \left[\lambda\gamma + \gamma(\phi - \lambda)e^{-\left(\frac{\delta}{x}\right)^{\eta}}\right]}{\left[1 - e^{-\left(\frac{\delta}{x}\right)^{\eta}}\right]^3} \exp\left\{-\lambda\left[e^{\left(\frac{\delta}{x}\right)^{\eta}} - 1\right]^{-1}\right.$$

$$\left. - \frac{\phi}{2}\left[e^{\left(\frac{\delta}{x}\right)^{\eta}} - 1\right]^{-2}\right\}$$

$$\times \left(1 - \exp\left\{ -\lambda \left[e^{\left(\frac{\delta}{x}\right)^{\eta}} - 1 \right]^{-1} - \frac{\phi}{2} \left[e^{\left(\frac{\delta}{x}\right)^{\eta}} - 1 \right]^{-2} \right\} \right)^{\gamma - 1}, \quad x > 0.$$

(9)

Henceforth, a random variable having PDF (9) will be denoted by $X \sim \text{GLFRF}(\lambda, \phi, \gamma, \delta, \eta)$. The GLFRF distribution is a very flexible distribution having several special sub-models. It contains 15 sub-models reported in Table 2.

Table 2: Special sub-models of the GLFRF distribution

λ	ϕ	γ	δ	η	Sub-model	Authors
-	-	1	δ	η	LFR-Fréchet	New
-	-	1	δ	1	LFR-inverse exponential	New
-	-	1	δ	2	LFR-inverse Rayleigh	New
0	-	-	δ	η	GR-Fréchet	New
0	-	-	δ	1	GR-inverse exponential	New
0	-	-	δ	2	GR-inverse Rayleigh	New
0	-	1	δ	η	Rayleigh-Fréchet	Bourguignon et al. (2014)
0	-	1	δ	1	Rayleigh-inverse exponential	-
0	-	1	δ	2	Rayleigh-inverse Rayleigh	-
-	0	1	δ	η	E-Fréchet	Bourguignon et al. (2014)
-	0	1	δ	η	E-inverse exponential	-
-	0	1	δ	η	E-inverse Rayleigh	-
-	0	-	δ	η	OGE-Fréchet	Tahir et al. (2015)
-	0	-	δ	η	OGE-inverse exponential	-
-	0	-	δ	η	OGE-inverse Rayleigh	-

Some possible shapes for the PDF and HRF of the GLFRF distribution are displayed in Figures 1 and 2 for different choices for the parameters $\lambda, \phi, \gamma, \delta$ and η. The plots show that the GLFRF model is very flexible in accommodating different hazard shapes especially non-monotone hazard rates including upside-down-bathtub (unimodal), bathtub and modified

bathtub shapes. The PDF plots of the GLFRF model show more flexibility. The HRF and RHRF of the GLFRF distribution take the form

$$h(x;\boldsymbol{\psi}) =$$

$$\frac{\eta\delta^{\eta}x^{-\eta-1}e^{-\left(\frac{\delta}{x}\right)^{\eta}}\left[1-e^{-\left(\frac{\delta}{x}\right)^{\eta}}\right]^{-3}\left[\lambda\gamma+\gamma(\phi-\lambda)e^{-\left(\frac{\delta}{x}\right)^{\eta}}\right]\exp\left\{-\lambda\left[e^{\left(\frac{\delta}{x}\right)^{\eta}}-1\right]^{-1}-\frac{\phi}{2}\left[e^{\left(\frac{\delta}{x}\right)^{\eta}}-1\right]^{-2}\right\}}{\left(1-\exp\left\{-\lambda\left[e^{\left(\frac{\delta}{x}\right)^{\eta}}-1\right]^{-1}-\frac{\phi}{2}\left[e^{\left(\frac{\delta}{x}\right)^{\eta}}-1\right]^{-2}\right\}\right)^{1-\theta}-\left(1-\exp\left\{-\lambda\left[e^{\left(\frac{\delta}{x}\right)^{\eta}}-1\right]^{-1}-\frac{\phi}{2}\left[e^{\left(\frac{\delta}{x}\right)^{\eta}}-1\right]^{-2}\right\}\right)}$$

(10)

and

$$\tau(x;\boldsymbol{\psi}) = \frac{\eta\delta^{\eta}x^{-\eta-1}e^{-\left(\frac{\delta}{x}\right)^{\eta}}\left[\lambda\gamma+\gamma(\phi-\lambda)e^{-\left(\frac{\delta}{x}\right)^{\eta}}\right]}{\left[1-e^{-\left(\frac{\delta}{x}\right)^{\eta}}\right]^{3}\left(\exp\left\{\lambda\left[e^{\left(\frac{\delta}{x}\right)^{\eta}}-1\right]^{-1}+\frac{\phi}{2}\left[e^{\left(\frac{\delta}{x}\right)^{\eta}}-1\right]^{-2}\right\}-1\right)}.$$
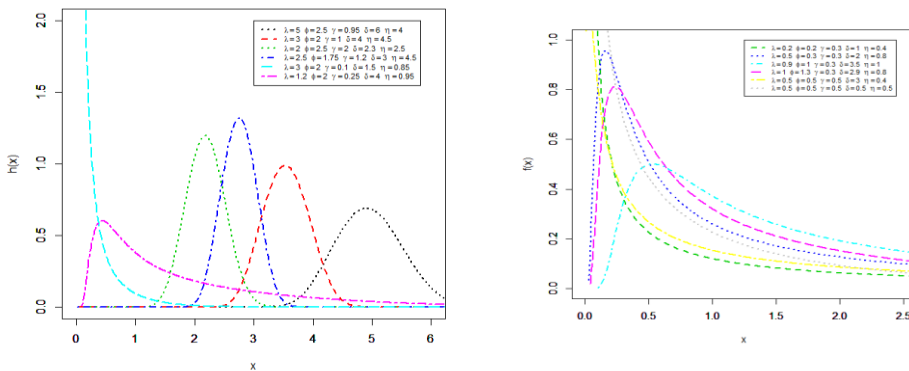
(11)

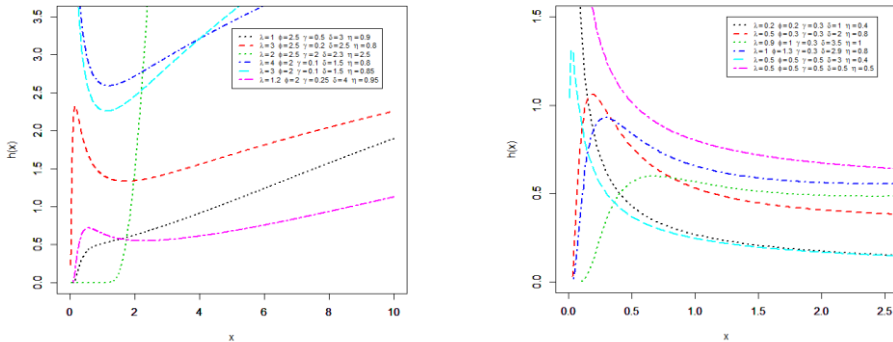Figure 1: Plots of the GLFRF PDF for some parameter values

Figure 2: Plots of the GLFRF HRF for some parameter values

The CHRF of the GLFRF distribution reduces to

$$H(x;\boldsymbol{\psi}) = -\log\left[1 - \left(1 - \exp\left\{-\lambda\left[e^{\left(\frac{\delta}{x}\right)^{\eta}} - 1\right]^{-1} - \frac{\phi}{2}\left[e^{\left(\frac{\delta}{x}\right)^{\eta}} - 1\right]^{-2}\right\}\right)^{\gamma}\right].$$

(12)

4. Linear Expansion

In this section, we provide a useful linear expansion for PDF of the GLFRF distribution. Afify et al. (2022) provided linear representations for the CDF and PDF of the GLFR-G family using the binomial and exponential series. The CDF and PDF of the GLFR-G family have the following linear expansions given by

$$F(x;\boldsymbol{\psi}) = \sum_{j,l=0}^{\infty}\sum_{k=0}^{j}\vartheta_{i,j,k,l}\,G(x)^{j+k+l}$$

and

$$f(x;\boldsymbol{\psi}) = \sum_{j,l=0}^{\infty}\sum_{k=0}^{j}\vartheta_{j,k,l}\,h_{J+k+l}(x),$$

(13)

where $\vartheta_{j,k,l} = \sum_{i=0}^{\infty}\left[(-1)^{i+j+l}(i\,\lambda)^{j}\phi^{k}\binom{\gamma}{i}\binom{j}{k}\binom{-j-k}{l}\right]/j!\,(2\,\lambda)^{k}$ and $h_{J+k+l}(x) = (j+k+l)\,g(x)\,G(x)^{j+k+l-1}$ is the exponentiated-G (exp-) PDF with power parameter $(j+k+l)$.

Using Equation (13) (Afify et al., 2022), we can provide a linear expansion of the PDF of the GLFRF distribution. By inserting Equations (6) and (7) of the Fréchet distribution in Equation (13), we obtain

$$f(x; \boldsymbol{\psi}) = \sum_{j,l=0}^{\infty} \sum_{k=0}^{j} \vartheta_{j,k,l} \, (j + k + l) \, \eta \delta^{\eta} x^{-\eta-1} \mathrm{e}^{-(j+k+l)\left(\frac{\delta}{x}\right)^{\eta}}.$$

Or equivalently, the above equation can be rewritten as

$$f(x; \boldsymbol{\psi}) = \sum_{j,l=0}^{\infty} \sum_{k=0}^{j} \vartheta_{j,k,l} \, g_{j+k+l}(x), \tag{14}$$

where $g_{j+k+l}(x)$ is the Fréchet PDF with shape parameter η and a scale parameter $\delta(j + k + l)^{1/\eta}$. Hence, the PDF of the GLFRF model may be expressed as a linear mixture of Fréchet densities. This, helps us to derive several properties of the GLFRF model using Equation (14) and the properties of the Fréchet distribution.

5. Mathematical Properties

In this section, some properties of the GLFRF distribution including quantile and generating functions, moments, and order statistics are derived.

5.1 Quantile and Generating Functions

The quantile function (QF) of the GLFRF distribution follows by inverting (8) as

$$Q(u) = \delta \left\{ -\log \left[\frac{-\lambda + \sqrt{\lambda^2 - 2\phi \log\left(1 - u^{\frac{1}{\gamma}}\right)}}{\phi - \lambda + \sqrt{\lambda^2 - 2\phi \log\left(1 - u^{\frac{1}{\gamma}}\right)}} \right] \right\}^{-1/\eta} , \quad 0 < u < 1.$$

The above equation can be used to simulate the GLFRF random variable. Particularly, if $u = 0.5$, we obtain of the median of the GLFRF distribution The moment generating function (MGF) of the Fréchet distribution defined by Equations (6) and (7), is denoted by $M(t; \delta, \eta)$. This MGF is derived by Afify et al. (2016) and using the formula of $M(t; \delta, \eta)$, we can obtain the MGF of the GLFRF distribution.

$$M(t; \delta, \eta) = \int_0^\infty \exp(t\,x) g(x) dx.$$

Let $w = 1/x$, we obtain

$$M(t; \delta, \eta) = \eta \delta^\eta \int_0^\infty \exp\left(\frac{t}{w}\right) w^{\eta-1} \exp[-(\delta w)^\eta] dw.$$

Using the exponential series for $\exp\left(\frac{t}{w}\right)$, it follows that

$$\exp\left(\frac{t}{w}\right) = \sum_{k=0}^\infty \frac{t^k}{k!} w^{-k}$$

Hence, we can write

$$M(t; \delta, \eta) = \eta \delta^\eta \sum_{k=0}^\infty \frac{t^k}{k!} \int_0^\infty w^{\eta-k-1} \exp[-(\delta w)^\eta] dw.$$

After some simplifications, we have

$$M(t; \delta, \eta) = \sum_{k=0}^\infty \frac{\delta^k\, t^k}{k!} \Gamma\left(\frac{\eta - k}{\eta}\right).$$

The Wright generalized hypergeometric function is defined by

$${}_p\Psi_q\left[\begin{matrix}(\delta_1, C_1), \ldots, (\delta_p, C_p) \\ (\eta_1, D_1), \ldots, (\eta_q, D_q)\end{matrix}; x\right] = \sum_{m=0}^\infty \frac{\prod_{i=1}^p \Gamma(\delta_i + C_i\, m)}{\prod_{i=1}^q \Gamma(\eta_i + D_i\, m)} \frac{x^m}{m!}.$$

Then, the MGF of the Fréchet distribution takes the form

$$M(t; \delta, \eta) = {}_1\Psi_0\left[\begin{matrix}(1, -\eta^{-1}); \\ \underline{\quad}\end{matrix} \delta t\right]. \tag{15}$$

Using Equations (14) and (15), we can write the MGF of the GLFRF distribution as follows

$$M_{GLFRF}(t) = \sum_{j,l=0}^\infty \sum_{k=0}^j \vartheta_{j,k,l}\, {}_1\Psi_0\left[\begin{matrix}(1, -\eta^{-1}); \\ \underline{\quad}\end{matrix} \delta\,(j + k + l)^{1/\eta}\, t\right].$$

5.2 Moments of the GLFRF Model

The rth ordinary moment of X is given by

$$\mu'_r = E(X^r) = \sum_{j,l=0}^{\infty} \sum_{k=0}^{j} \vartheta_{j,k,l} \int_0^{\infty} x^r \, g_{j+k+l}(x)dx.$$

For $r < \eta$, we have

$$\mu'_r = \sum_{j,l=0}^{\infty} \sum_{k=0}^{j} \vartheta_{j,k,l} \, \delta^r \, (j+k+l)^{r/\eta} \, \Gamma\left(1 - \frac{r}{\eta}\right).$$

The mean of X follows for $r = 1$ in the above formula, that is

$$\mu'_1 = \sum_{j,l=0}^{\infty} \sum_{k=0}^{j} \vartheta_{j,k,l} \, \delta \, (j+k+l)^{1/\eta} \, \Gamma\left(1 - \frac{1}{\eta}\right).$$

The rth incomplete moment is defined by

$$\varphi_r(t) = \int_0^t x^r \, f(x)dx.$$

Using Equation (14), we have

$$\varphi_r(t) = \sum_{j,l=0}^{\infty} \sum_{k=0}^{j} \vartheta_{j,k,l} \int_0^t x^r \, g_{j+k+l}(x)dx.$$

The rth incomplete moment of the GLFRF distribution follows (for $r < \eta$) as

$$\varphi_r(t) = \sum_{j,l=0}^{\infty} \sum_{k=0}^{j} \vartheta_{j,k,l} \, \delta^r (j+k+l)^{\frac{r}{\eta}} \gamma\left(1 - \frac{r}{\eta}, (j+k+l)\left(\frac{\delta}{t}\right)^{\eta}\right).$$

For $r = 1$, the first incomplete moment (FIM) follows as

$$\varphi_1(t) = \sum_{j,l=0}^{\infty} \sum_{k=0}^{j} \vartheta_{j,k,l} \, \delta(j+k+l)^{\frac{1}{\eta}} \gamma\left(1 - \frac{1}{\eta}, (j+k+l)\left(\frac{\delta}{t}\right)^{\eta}\right).$$

FIM can be used to calculate the mean residual life (MRL), $m_1(t) = [1 - \varphi_1(t)]/S(t) - t$, and the mean inactivity time (MIT), $M_1(t) = t - \varphi_1(t)/F(t)$. The MRL has applications in some fields such as biomedical

sciences, survival analysis, life insurance, product quality control, economics, product technology, and demography (Lai and Xie, 2006).

5.3 Residual and Reversed Residual Lifes

The sth moments of residual life is given (for $s = 1,2,3,...$) by

$$m_s(t) = E((X - t)^s | X > t) = \frac{1}{1 - F(t)} \int_t^\infty (x - t)^s dF(x).$$

Then, $m_s(t)$ of the GLFRF distribution follows (for $s < \eta$) as

$$m_s(t) = \frac{1}{1 - F(t)} \sum_{r=0}^{s} \frac{(-1)^{s-r} \Gamma(s+1)}{r! \, \Gamma(s - r + 1)} t^{s-r} \delta^r \sum_{j,l=0}^{\infty} \sum_{k=0}^{j} \vartheta_{j,k,l} \, (j + k + l)^{\frac{r}{\eta}}$$

$$\times \Gamma\left(1 - \frac{r}{\eta}, (j + k + l)\left(\frac{\delta}{t}\right)^\eta\right),$$

where $F(t)$ is the CDF of the GLFRF model and $\Gamma(z, a) = \int_a^\infty w^{z-1} e^{-w} dw$ is the the upper incomplete GF. The MRL of the GLFRF distribution follows by setting $s = 1$ in the above equation.

The sth moments of the reversed residual life (RRL) is defined (for $s = 1,2,3,...$) by

$$M_s(t) = E((t - X)^s | X \leq t) = \frac{1}{F(t)} \int_0^t (t - x)^s dF(x)..$$

The sth moments of the RRL of the GLFRF distribution reduces to (for $s < \eta$)

$$M_s(t) = \frac{1}{F(t)} \sum_{r=0}^{s} \frac{(-1)^r \Gamma(s+1)}{r! \, \Gamma(s - r + 1)} t^{s-r} \delta^r \sum_{j,l=0}^{\infty} \sum_{k=0}^{j} \vartheta_{j,k,l} \, (j + k + l)^{\frac{r}{\eta}}$$

$$\times \gamma\left(1 - \frac{r}{\eta}, (j + k + l)\left(\frac{\delta}{t}\right)^\eta\right).$$

The mean waiting time (MWT) or mean reversed residual life of the GLFRF distribution follows by setting $s = 1$ in the lsat equation.

5.4 Order Statistics

Consider the random sample of size n, $X_1, ..., X_n$, from the GLFRF distribution. Then, the corresponding order statistics are $X_{(1)}, ..., X_{(n)}$. The PDF of the ith order statistic $X_{i:n}$, $f_{i:n}(x)$, is defined as

$$f_{i:n}(x; \boldsymbol{\psi})$$

$$= \sum_{q=0}^{n-i} \frac{(-1)^q \binom{n-i}{q}}{B(i, n-i+1)} f(x; \boldsymbol{\psi})\, F(x; \boldsymbol{\psi})^{i+q-1}. \tag{16}$$

Afify et al. (2022) derived a general formula for $f_{i:n}(x)$, of the GLFR-G family as

$$f_{i:n}(x; \boldsymbol{\psi})$$

$$= \sum_{q=0}^{n-i} \frac{(-1)^q \binom{n-i}{q}}{B(i, n-i+1)} \frac{\lambda \gamma g(x; \boldsymbol{\psi}) + \gamma(\phi - \lambda) g(x; \boldsymbol{\psi}) G(x; \boldsymbol{\psi})}{[1 - G(x; \boldsymbol{\psi})]^3} \exp\left\{ -\lambda \left[\frac{G(x; \boldsymbol{\psi})}{1 - G(x; \boldsymbol{\psi})} \right] \right.$$

$$\left. - \frac{\phi}{2} \left[\frac{G(x; \boldsymbol{\psi})}{1 - G(x; \boldsymbol{\psi})} \right]^2 \right\}$$

$$\times \left(1 - \exp\left\{ -\lambda \left[\frac{G(x; \boldsymbol{\psi})}{1 - G(x; \boldsymbol{\psi})} \right] \right.\right.$$

$$\left.\left. - \frac{\phi}{2} \left[\frac{G(x; \boldsymbol{\psi})}{1 - G(x; \boldsymbol{\psi})} \right]^2 \right\} \right)^{\gamma(i+q)-1} \tag{17}$$

Substituting (6) and (7) in Equation (17), we obtian the PDF for the ith order statistic of the GLFRF distribution

$$f_{i:n}(x; \boldsymbol{\psi})$$

$$= \sum_{q=0}^{n-i} \frac{(-1)^q \binom{n-i}{q}}{B(i, n-i+1)} \frac{\eta \delta^\eta x^{-\eta-1} e^{-\left(\frac{\delta}{x}\right)^\eta} \left[\lambda \gamma + \gamma(\phi - \lambda) e^{-\left(\frac{\delta}{x}\right)^\eta} \right]}{\left[1 - e^{-\left(\frac{\delta}{x}\right)^\eta} \right]^3} \exp\left\{ -\lambda \left[e^{\left(\frac{\delta}{x}\right)^\eta} \right.\right.$$

$$\left.\left. - 1 \right]^{-1} - \frac{\phi}{2} \left[e^{\left(\frac{\delta}{x}\right)^\eta} - 1 \right]^{-2} \right\}$$

$$\times \left(1 - \exp\left\{ -\lambda \left[e^{\left(\frac{\delta}{x}\right)^\eta} - 1 \right]^{-1} \right.\right.$$

$$\left.\left. - \frac{\phi}{2} \left[e^{\left(\frac{\delta}{x}\right)^\eta} - 1 \right]^{-2} \right\} \right)^{\gamma(i+q)-1} \tag{18}$$

Applying the binomial expansion to the last term in (18), it follows that

$$\sum_{l=0}^{\infty} (-1)^l \binom{\gamma(i+q)-1}{l} \left(\exp\left\{-\lambda\left[e^{\left(\frac{\delta}{x}\right)^{\eta}} - 1\right]^{-1} - \frac{\phi}{2}\left[e^{\left(\frac{\delta}{x}\right)^{\eta}} - 1\right]^{-2}\right\}\right)^l.$$

Hence, Equation (18) reduces to

$$f_{i:n}(x; \boldsymbol{\psi}) = \sum_{l=0}^{\infty} v_{q,i}\, \eta \delta^{\eta} x^{-\eta-1} e^{-\left(\frac{\delta}{x}\right)^{\eta}} \left[\lambda\gamma + \gamma(\phi - \lambda)e^{-\left(\frac{\delta}{x}\right)^{\eta}}\right]\left[1 - e^{-\left(\frac{\delta}{x}\right)^{\eta}}\right]^{-3}$$

$$\times \exp\left\{-\lambda(l+1)\left[e^{\left(\frac{\delta}{x}\right)^{\eta}} - 1\right]^{-1} - \frac{\phi(l+1)}{2}\left[e^{\left(\frac{\delta}{x}\right)^{\eta}} - 1\right]^{-2}\right\},$$

where $v_{q,i} = \sum_{q=0}^{n-i} \frac{(-1)^{q+l}\binom{n-i}{q}}{B(i,n-i+1)}\binom{\gamma(i+q)-1}{l}$.

6. Maximum Likelihood Estimation

In this section, the five parameters of the GLFRF distribution are estimated using the maximum likelihood (ML) approach. Let $x_1, \ldots, x_n$ be a random sample from the GLFRF distribution with an unknown vector of parameters $\boldsymbol{\psi} = (\lambda, \phi, \gamma, \delta, \eta)^T$.

The log-likelihood function for $\boldsymbol{\psi}$ takes the form

$$\ell = n(\log\eta + \eta\log\delta) - (\eta+1)\sum_{i=1}^{n}\log x_i - \sum_{i=1}^{n}\left(\frac{\delta}{x_i}\right)^{\eta}$$

$$- 3\sum_{i=1}^{n}\log\left(1 - e^{-\left(\frac{\delta}{x_i}\right)^{\eta}}\right) + \sum_{i=1}^{n}\log\left[\lambda\gamma + \gamma(\phi - \lambda)e^{-\left(\frac{\delta}{x_i}\right)^{\eta}}\right]$$

$$- \lambda\sum_{i=1}^{n}(s_i - 1)^{-1} - \frac{\phi}{2}\sum_{i=1}^{n}(s_i - 1)^{-2}$$

$$+ (\gamma - 1)\sum_{i=1}^{n}\log\left(1 - \exp\left[-\lambda(s_i - 1)^{-1} - \frac{\phi}{2}(s_i - 1)^{-2}\right]\right),$$

where $s_i = e^{\left(\frac{\delta}{x_i}\right)^{\eta}}$.

The above log-likelihood can be maximized by solving the nonlinear likelihood equations semultaniously or using the statistical software such as R, SAS, Mathemtica and Matlab.

The nonlinear likelihood equations follow by differentiating ℓ with respect to all parameters. That is, the score vector elements, $\mathbf{U}(\boldsymbol{\psi}) = \frac{\partial \ell}{\partial \boldsymbol{\psi}} = (\frac{\partial \ell}{\partial \lambda}, \frac{\partial \ell}{\partial \phi}, \frac{\partial \ell}{\partial \gamma}, \frac{\partial \ell}{\partial \delta}, \frac{\partial \ell}{\partial \eta})^T$, are

$$\frac{\partial \ell}{\partial \lambda} = \sum_{i=1}^{n} \frac{\gamma(s_i - 1)}{\lambda \gamma s_i + \gamma(\phi - \lambda)} - \sum_{i=1}^{n} (s_i - 1)^{-1} + (\gamma - 1) \sum_{i=1}^{n} \frac{(s_i - 1)^{-1} K_i}{1 - K_i},$$

$$\frac{\partial \ell}{\partial \phi} = \sum_{i=1}^{n} \frac{\gamma}{\lambda \gamma s_i + \gamma(\phi - \lambda)} - \frac{1}{2} \sum_{i=1}^{n} (s_i - 1)^{-2} + \frac{(\gamma - 1)}{2} \sum_{i=1}^{n} \frac{(s_i - 1)^{-2} K_i}{1 - K_i}$$

$$\frac{\partial \ell}{\partial \gamma} = \sum_{i=1}^{n} \frac{\lambda s_i + (\phi - \lambda)}{\lambda \gamma s_i + \gamma(\phi - \lambda)} + \sum_{i=1}^{n} \log(1 - K_i),$$

$$\frac{\partial \ell}{\partial \delta} = \frac{n\eta}{\delta} - \frac{\eta}{\delta} \sum_{i=1}^{n} \left(\frac{\delta}{x_i}\right)^{\eta} - \frac{3\eta}{\delta} \sum_{i=1}^{n} \frac{\left(\frac{\delta}{x_i}\right)^{\eta}}{s_i - 1} + \frac{\lambda \eta}{\delta} \sum_{i=1}^{n} \left(\frac{\delta}{x_i}\right)^{\eta} \frac{s_i}{(s_i - 1)^2}$$
$$- \frac{\eta}{\delta} \sum_{i=1}^{n} \frac{\gamma(\phi - \lambda)\left(\frac{\delta}{x_i}\right)^{\eta}}{\lambda \gamma s_i + \gamma(\phi - \lambda)} + \frac{\phi \eta}{\delta} \sum_{i=1}^{n} \left(\frac{\delta}{x_i}\right)^{\eta} \frac{s_i}{(s_i - 1)^3}$$
$$- \frac{\eta(\gamma - 1)}{\delta} \sum_{i=1}^{n} \frac{s_i[\lambda + \phi(s_i - 1)^{-1}]}{(\delta/x_i)^{-\eta}(s_i - 1)^2} \frac{K_i}{(1 - K_i)}$$

and

$$\frac{\partial \ell}{\partial \eta} = \frac{n}{\eta} + n \log \delta - \sum_{i=1}^{n} \log x_i - \sum_{i=1}^{n} \left(\frac{\delta}{x_i}\right)^{\eta} \log\left(\frac{\delta}{x_i}\right)$$

$$- 3 \sum_{i=1}^{n} \frac{\log\left(\frac{\delta}{x_i}\right)}{(\delta/x_i)^{-\eta}(s_i - 1)} - \sum_{i=1}^{n} \frac{\left(\frac{\delta}{x_i}\right)^{\eta} \log\left(\frac{\delta}{x_i}\right)}{\lambda \gamma s_i + \gamma(\phi - \lambda)}$$

$$+ \lambda \sum_{i=1}^{n} \frac{s_i \log\left(\frac{\delta}{x_i}\right)}{(\delta/x_i)^{-\eta}(s_i - 1)^2} + \phi \sum_{i=1}^{n} \frac{s_i \log\left(\frac{\delta}{x_i}\right)}{(\delta/x_i)^{-\eta}(s_i - 1)^3}$$

$$- (\gamma - 1) \sum_{i=1}^{n} \frac{s_i \log\left(\frac{\delta}{x_i}\right) [\lambda + \phi(s_i - 1)^{-1}]}{(\delta/x_i)^{-\eta}(s_i - 1)^2} \frac{K_i}{(1 - K_i)},$$

where $K_i = \exp\left[-\lambda(s_i - 1)^{-1} - \frac{\phi}{2}(s_i - 1)^{-2}\right]$

The ML estimates (MLEs) of the GLFRF parameters can be obtained by setting $\mathbf{U}(\widehat{\boldsymbol{\psi}}) = \mathbf{0}$. Solving these five equations simultaneously yields the MLEs $\hat{\lambda}, \hat{\phi}, \hat{\gamma}, \hat{\delta}$ and $\hat{\eta}$. Additionally, the MLEs can be determined numerically using iterative techniques like the Newton-Raphson algorithm.

7. Simulation Results

The behaviour of the MLEs of the GLFRF parameters are investigated in this section using some numerical simulations in terms of the sample size n. The GLFRF distribution is simulated using its QF given in Section 5.1.

Using the software R programming language R (R Core Team, 2020), 4,000 random samples from the GLFRF distribution are generated with four sample sizes $n = 30, 50, 200$ and $n = 500$. The true values of the GLFRF parameters are selected as follows: $\lambda = (0.4, 1.0, 3.5)$, $\phi = (0.5, 1.0, 4.7)$, $\gamma = (0.6, 1.0, 2.9)$, $\delta = (0.2, 1.0, 2.1)$ and $\eta = (0.2, 1.0, 2.1)$. Tables 3-9 illustrate the averages of the following quantities: mean square errors (MSE), $\text{MSE}(\widehat{\boldsymbol{\psi}}) = \frac{1}{N}\sum_{i=1}^{N}(\widehat{\boldsymbol{\psi}}_i - \boldsymbol{\psi})^2$, absolute biases (ABB), $\text{ABB}(\widehat{\boldsymbol{\psi}}) = \frac{1}{N}\sum_{i=1}^{N}|\widehat{\boldsymbol{\psi}}_i - \boldsymbol{\psi}|$, and mean relative estimates (MRE), $\text{MRE}(\widehat{\boldsymbol{\psi}}) = \frac{1}{N}\sum_{i=1}^{N}|\widehat{\boldsymbol{\psi}}_i - \boldsymbol{\psi}|/\boldsymbol{\psi}$. These measures are calculated for all sample sizes and all parameters' combinations. These tables show that the MLEs of the GLFRF parameters are stable and consistent. Additionally, these tables reveal that the

MSE, ABB, and MRE of the parameters decay toward zero as the sample size increases.

8. Two Real-life Data Applications

This section is devoted to explore the empirical importance of the GLFRF distribution using two real-life data applications. The first set of data from Smith and Naylor (1987) consists of 63 observations about strengths of 1.5 cm glass fibres which are measured at National-Physical-Laboratory, in England. The observations are: 0.55, 1.25, 0.93, 1.49, 1.36, 1.52, 1.61, 1.58, 1.64, 1.73, 0.77, 1.68, 1.81, 1.27, 0.74, 2, 1.04, 1.39, 1.53, 1.49, 1.59, 1.66, 1.61, 1.68, 1.82, 1.76, 1.11, 2.01, 1.28, 1.42, 1.54, 1.5, 1.6, 1.66, 1.69, 1.62, 1.76, 2.24, 1.84, 0.81, 1.29, 1.13, 1.48, 1.55, 1.5, 1.61, 1.66, 1.55, 1.7, 1.62, 1.77, 0.84, 1.84, 1.24, 1.51, 1.48, 1.63, 1.61, 1.67, 1.78, 1.7, 1.89, 1.3. This data are studied by Barreto-Souza et al. (2011) and Afify et al. (2015).

The second set of data consists of 72 exceedances flood peaks for the years 1958-1984, rounded to one decimal place. These flood peaks (in m3/s) measures for Wheaton river in Canada. The data are 0.4, 1.7, 14.4, 2.2, 1.1, 5.3, 0.7, 1.9, 13.0, 12.0, 9.3, 1.4, 18.7, 8.5, 25.5, 11.6, 14.1, 1.1, 2.5, 14.4, 1.7, 2.2, 37.6, 0.6, 39.0, 22.1, 0.3, 15.0, 11.0, 7.3, 22.9, 1.7, 1.1, 0.1, 0.6, 1.7, 9.0, 7.0, 0.4, 20.1, 2.8, 9.9, 14.1, 10.4, 30.0, 10.7, 3.6, 5.6, 30.8, 13.3, 4.2, 3.4, 25.5, 11.9, 27.6, 21.5, 36.4, 64.0, 2.7, 1.5, 27.4, 2.5, 1.0, 20.2, 27.1, 5.3, 16.8, 2.5, 9.7, 27.0, 20.6, 27.5.

The fit of the GLFRF distribution is compared with some competing distribution such as the Kumaraswamy-Fréchet (KF), Kumaraswamy-Marshall-Olkin Fréchet (KMOF), beta-Fréchet (BF), exponentiated-Fréchet (EF), gamma extended-Fréchet (GEF), transmuted-Fréchet (TF) and Fréchet (F) distributions. The corresponding PDFs of these competing moels are given by (for $x > 0$)

Table 3: Simulation results of the GLFRF distribution for several parametric values

λ	ϕ	γ	δ	λ	n		$\hat{\lambda}$	$\hat{\phi}$	$\hat{\gamma}$	$\hat{\delta}$	$\hat{\eta}$
0.4	1.5	0.6	1.2	1.5	30	MSE	0.16103	0.72245	0.17188	0.49396	0.46224
						ABB	0.36105	0.80002	0.35239	0.64230	0.59792

λ	φ	γ	δ	λ	n		$\hat{\lambda}$	$\hat{\phi}$	$\hat{\gamma}$	$\hat{\delta}$	$\hat{\eta}$
						MRE	0.90263	0.80002	0.58732	0.53525	0.79722
					50	MSE	0.15328	0.70017	0.16078	0.45922	0.36103
						ABB	0.34594	0.77907	0.32726	0.61182	0.50809
						MRE	0.86485	0.77907	0.54543	0.50985	0.67745
					200	MSE	0.09799	0.60965	0.08569	0.38954	0.23229
						ABB	0.27472	0.70079	0.23472	0.54715	0.37515
						MRE	0.68681	0.70079	0.39120	0.45596	0.50020
					500	MSE	0.07520	0.60043	0.06724	0.37527	0.20527
						ABB	0.24017	0.68609	0.21112	0.53106	0.33160
						MRE	0.60041	0.68609	0.35187	0.44255	0.44213
					30	MSE	0.17001	0.71689	0.16830	0.19630	0.70663
						ABB	0.35579	0.78772	0.33540	0.38685	0.78351
						MRE	0.88948	0.78772	0.55900	0.32238	0.52234
					50	MSE	0.15285	0.70903	0.15562	0.18390	0.60633
						ABB	0.34075	0.78291	0.32031	0.37626	0.70942
1.5	0.5	1.5	2.5	1.5		MRE	0.85188	0.78291	0.53385	0.31355	0.47295
					200	MSE	0.10548	0.65707	0.10128	0.17043	0.35042
						ABB	0.28987	0.71352	0.25717	0.35960	0.49428
						MRE	0.72468	0.69352	0.42862	0.29967	0.32952
					500	MSE	0.25036	0.78291	0.07034	0.16788	0.25297
						ABB	0.25036	0.63471	0.21992	0.35245	0.39288
						MRE	0.62590	0.59471	0.36654	0.29371	0.26192

λ	ϕ	γ	δ	λ	n			$\hat{\lambda}$	$\hat{\phi}$	$\hat{\gamma}$	$\hat{\delta}$	$\hat{\eta}$
0.4	1.5	0.6	1.2	1.5	30	MSE		0.18104	0.74979	0.16606	0.20086	0.70859
						ABB		0.36384	0.05116	0.32810	0.39300	0.78530
						MRE		0.90959	0.70077	0.54683	0.32750	0.52354
					50	MSE		0.16141	0.70079	0.16031	0.19339	0.61292
						ABB		0.34972	0.07914	0.32608	0.38486	0.71151
						MRE		0.87431	0.65943	0.54347	0.32072	0.47434
					200	MSE		0.11676	0.67936	0.12630	0.18247	0.36769
						ABB		0.30171	0.08208	0.28709	0.37074	0.50999
						MRE		0.75429	0.59139	0.47848	0.30895	0.34000
					500	MSE		0.07883	0.59273	0.08830	0.16858	0.24867
						ABB		0.24974	0.06596	0.23994	0.34706	0.39017
						MRE		0.62436	0.45106	0.39990	0.28922	0.26011

Table 4: Simulation results of the GLFRF distribution for several parametric values

λ	ϕ	γ	δ	λ	n			$\hat{\lambda}$	$\hat{\phi}$	$\hat{\gamma}$	$\hat{\delta}$	$\hat{\eta}$
1.5	0.5	1.5	2.5	1.5	30	MSE		0.95795	0.43582	0.99569	0.55573	0.71039
						ABB		0.88573	0.58288	0.95895	0.61925	0.76837
						MRE		0.59049	0.66577	0.63930	0.24770	0.51225
					50	MSE		0.87838	0.41723	0.90058	0.51642	0.65122
						ABB		0.83986	0.57039	0.89415	0.60572	0.72845
						MRE		0.55991	0.64078	0.59610	0.21429	0.48564
					200	MSE		0.69347	0.40654	0.56832	0.49018	0.43995
						ABB		0.74086	0.53263	0.67527	0.55275	0.57386

λ	ϕ	γ	δ	λ	n		$\hat{\lambda}$	$\hat{\phi}$	$\hat{\gamma}$	$\hat{\delta}$	$\hat{\eta}$
						MRE	0.49391	0.54527	0.45018	0.20710	0.38257
					500	MSE	0.60998	0.32018	0.41045	0.45816	0.30993
						ABB	0.69173	0.42042	0.55753	0.42558	0.46532
						MRE	0.46115	0.38085	0.37169	0.18423	0.31021
0.75	0.5	1.5	2.5	1.5	30	MSE	0.31985	0.23277	0.81988	0.79660	0.73673
						ABB	0.49626	0.41175	0.85946	0.77226	0.79406
						MRE	0.66168	0.82349	0.57297	0.30891	0.52937
					50	MSE	0.28773	0.21578	0.75647	0.69550	0.66650
						ABB	0.47039	0.40566	0.81289	0.70435	0.74353
						MRE	0.62719	0.75133	0.54193	0.28174	0.49568
					200	MSE	0.20948	0.18562	0.42736	0.54646	0.43866
						ABB	0.39806	0.35529	0.57099	0.61573	0.56621
						MRE	0.53075	0.65059	0.38066	0.24629	0.37747
					500	MSE	0.30568	0.75133	0.24698	0.44283	0.34300
						ABB	0.30568	0.29108	0.41006	0.55608	0.47597
						MRE	0.39424	0.52217	0.27337	0.20843	0.31731
0.75	0.5	1.5	2.5	3.5	30	MSE	0.41723	0.62215	0.67028	0.24262	0.88713
						ABB	0.56198	0.71754	0.76213	0.41163	0.90539
						MRE	0.74930	0.43509	0.50809	0.16465	0.25868
					50	MSE	0.37920	0.58559	0.65301	0.23101	0.86047
						ABB	0.52962	0.68586	0.75364	0.39862	0.88711
						MRE	0.70616	0.37172	0.50243	0.15945	0.25346

λ	ϕ	γ	δ	λ	n		$\hat{\lambda}$	$\hat{\phi}$	$\hat{\gamma}$	$\hat{\delta}$	$\hat{\eta}$
					200	MSE	0.21538	0.48016	0.45294	0.15997	0.76675
						ABB	0.38789	0.60361	0.58824	0.32725	0.81773
						MRE	0.51719	0.20721	0.39216	0.13090	0.23364
					500	MSE	0.16132	0.44568	0.29252	0.12719	0.62689
						ABB	0.33866	0.58072	0.44598	0.29663	0.71411
						MRE	0.45155	0.16143	0.29732	0.11865	0.20403

Table 5: Simulation results of the GLFRF distribution for several parametric values

λ	ϕ	γ	δ	λ	n		$\hat{\lambda}$	$\hat{\phi}$	$\hat{\gamma}$	$\hat{\delta}$	$\hat{\eta}$
0.4	0.5	1.5	2.5	3.5	30	MSE	0.30665	0.62961	0.56832	0.33140	0.88463
						ABB	0.44897	0.72442	0.69152	0.48791	0.91098
						MRE	0.90242	0.44885	0.46102	0.19517	0.26028
					50	MSE	0.29084	0.56968	0.54755	0.31897	0.84018
						ABB	0.43434	0.67566	0.67480	0.47728	0.87428
						MRE	0.88584	0.35132	0.44987	0.19091	0.24979
					200	MSE	0.13443	0.46020	0.43353	0.25323	0.63107
						ABB	0.29229	0.57966	0.58084	0.40706	0.71316
						MRE	0.73073	0.15933	0.38723	0.16283	0.20376
					500	MSE	0.07366	0.41082	0.30114	0.16832	0.46999
						ABB	0.22138	0.53894	0.46158	0.33591	0.58363
						MRE	0.55345	0.07788	0.30772	0.13436	0.16675
0.4	1	1.5	2.5	3.5	30	MSE	0.31837	0.87893	0.51842	0.25930	0.88002
						ABB	0.46245	0.91342	0.65596	0.39751	0.91021

λ	φ	γ	δ	λ	n		λ̂	φ̂	γ̂	δ̂	η̂
						MRE	0.89612	0.91342	0.43731	0.15901	0.26006
					50	MSE	0.32427	0.83080	0.49372	0.26414	0.84237
						ABB	0.46738	0.87959	0.63333	0.40744	0.87951
						MRE	0.86844	0.87959	0.42222	0.16298	0.25129
					200	MSE	0.20374	0.72267	0.43065	0.25617	0.62622
						ABB	0.36467	0.79897	0.58010	0.40087	0.71041
						MRE	0.71168	0.79897	0.38673	0.16035	0.20297
					500	MSE	0.27103	0.87959	0.36354	0.21643	0.45314
						ABB	0.27103	0.77833	0.51603	0.36884	0.56574
						MRE	0.67757	0.77833	0.34402	0.14754	0.16164
					30	MSE	0.78393	0.57618	0.80593	0.01549	0.84973
						ABB	0.80349	0.65282	0.85504	0.09579	0.88000
						MRE	0.53566	2.61127	0.57003	0.12772	0.25143
					50	MSE	0.70689	0.50523	0.78187	0.01437	0.82882
						ABB	0.75884	0.59716	0.83816	0.09639	0.86509
1.5	0.25	0.75	0.75	3.5		MRE	0.50590	2.38864	0.55877	0.12852	0.24717
					200	MSE	0.52946	0.40548	0.60751	0.01097	0.70359
						ABB	0.64114	0.51170	0.70448	0.08695	0.77188
						MRE	0.42743	2.04679	0.46965	0.11594	0.22054
					500	MSE	0.51100	0.32190	0.46080	0.00916	0.60529
						ABB	0.50227	0.44241	0.58919	0.08110	0.70057
						MRE	0.42818	1.76964	0.39279	0.10813	0.20016

Table 6: Simulation results of the GLFRF distribution for several parametric values

λ	ϕ	γ	δ	λ	n		$\hat{\lambda}$	$\hat{\phi}$	$\hat{\gamma}$	$\hat{\delta}$	$\hat{\eta}$
1.5	0.25	0.75	1.2	1.5	30	MSE	0.96637	0.46361	1.06941	0.22900	0.69567
						ABB	0.90037	0.56010	0.99165	0.38274	0.76250
						MRE	0.60025	0.89041	0.61110	0.31895	0.50833
					50	MSE	0.86028	0.41935	0.98050	0.22245	0.60955
						ABB	0.84728	0.52721	0.93804	0.37453	0.70080
						MRE	0.56485	0.79885	0.62536	0.31211	0.46720
					200	MSE	0.66065	0.35081	0.63413	0.14574	0.35794
						ABB	0.73157	0.47406	0.72311	0.30432	0.50429
						MRE	0.48771	0.65622	0.48207	0.25360	0.33619
					500	MSE	0.62113	0.32150	0.46753	0.12769	0.23812
						ABB	0.71464	0.45258	0.60265	0.29879	0.40180
						MRE	0.47643	0.55032	0.40176	0.24899	0.26786
0.4	0.25	1.5	1.2	1.5	30	MSE	0.15473	0.19557	0.85860	0.46377	0.74351
						ABB	0.32272	0.33013	0.87959	0.57678	0.80062
						MRE	0.80681	0.72054	0.58639	0.48065	0.53375
					50	MSE	0.14484	0.19404	0.76151	0.41190	0.64605
						ABB	0.30870	0.33052	0.81322	0.53294	0.72620
						MRE	0.77175	0.52207	0.54215	0.44412	0.48413
					200	MSE	0.08567	0.17708	0.39836	0.23038	0.38845
						ABB	0.24841	0.29008	0.54600	0.38556	0.51757
						MRE	0.62103	0.32034	0.36400	0.32130	0.34504

λ	φ	γ	δ	λ	n						
					500	MSE	0.22451	0.52207	0.23791	0.19935	0.27970
						ABB	0.22451	0.22240	0.40628	0.32597	0.40968
						MRE	0.56127	0.29958	0.27086	0.31331	0.27312
0.75	0.5	0.75	0.25	0.5	30	MSE	0.43989	0.27442	1.12058	0.15811	0.41045
						ABB	0.62538	0.47480	1.00912	0.27479	0.54073
						MRE	0.83384	0.94960	0.67274	1.09918	1.08146
					50	MSE	0.38436	0.31129	0.90824	0.13738	0.28934
						ABB	0.57355	0.50212	0.88768	0.25021	0.43487
						MRE	0.76473	1.00425	0.59178	1.00083	0.86975
					200	MSE	0.28347	0.41236	0.46419	0.08835	0.09973
						ABB	0.47689	0.57271	0.60113	0.21287	0.24121
						MRE	0.63585	1.14542	0.40075	0.85149	0.48242
					500	MSE	0.21721	0.44119	0.26095	0.06220	0.05841
						ABB	0.40914	0.59294	0.42849	0.19502	0.18208
						MRE	0.54552	1.18588	0.28566	0.78006	0.36416

Table 7: Simulation results of the GLFRF distribution for several parametric values

λ	φ	γ	δ	λ	n		$\hat{\lambda}$	$\hat{\phi}$	$\hat{\gamma}$	$\hat{\delta}$	$\hat{\eta}$
0.75	0.5	0.75	0.5	0.5	30	MSE	0.43474	0.25760	1.08257	0.26816	0.43179
						ABB	0.62224	0.47373	0.99241	0.40337	0.55290
						MRE	0.82966	0.94745	0.66161	0.80675	1.10580
					50	MSE	0.37366	0.26983	0.87526	0.24351	0.29892
						ABB	0.56471	0.47352	0.87307	0.38226	0.44042
						MRE	0.75295	0.94705	0.58204	0.76452	0.88084

λ	ϕ	γ	δ	λ	n		$\hat{\lambda}$	$\hat{\phi}$	$\hat{\gamma}$	$\hat{\delta}$	$\hat{\eta}$
					200	MSE	0.25786	0.33902	0.44361	0.20880	0.09975
						ABB	0.45194	0.51306	0.58850	0.36069	0.24001
						MRE	0.60259	1.02612	0.39233	0.72137	0.48001
					500	MSE	0.20249	0.38558	0.25020	0.19130	0.05793
						ABB	0.39277	0.54982	0.42133	0.35643	0.18065
						MRE	0.52369	1.09964	0.28089	0.71286	0.36129
0.75	1.5	0.6	0.25	0.75	30	MSE	0.43090	1.09595	0.21573	0.06674	0.36688
						ABB	0.60999	0.84908	0.40288	0.18542	0.51988
						MRE	0.81331	0.56605	0.67146	0.74169	0.69317
					50	MSE	0.39053	1.13569	0.18035	0.07057	0.27527
						ABB	0.57289	0.88159	0.35697	0.18583	0.43972
						MRE	0.76385	0.58773	0.59496	0.74331	0.58629
					200	MSE	0.29184	1.20793	0.11293	0.10248	0.15695
						ABB	0.47820	0.94092	0.26681	0.20608	0.31228
						MRE	0.63760	0.62728	0.44469	0.82433	0.41638
					500	MSE	0.40462	0.58773	0.06954	0.11470	0.12851
						ABB	0.40462	0.96429	0.21227	0.21756	0.26847
						MRE	0.53949	0.64286	0.35378	0.87023	0.35797
0.75	1	0.75	0.5	0.5	30	MSE	0.43216	0.75756	0.95651	0.26758	0.48035
						ABB	0.61840	0.83019	0.99321	0.40466	0.59506
						MRE	0.82453	0.83019	0.66214	0.80933	0.97012
					50	MSE	0.41035	0.75831	0.92219	0.22199	0.34105

λ	ϕ	γ	δ	λ	n		$\hat{\lambda}$	$\hat{\phi}$	$\hat{\gamma}$	$\hat{\delta}$	$\hat{\eta}$
						ABB	0.59620	0.82695	0.89840	0.36633	0.47787
						MRE	0.79493	0.82695	0.59893	0.73266	0.95574
					200	MSE	0.28779	0.72067	0.46928	0.16225	0.11180
						ABB	0.47997	0.78990	0.59921	0.32991	0.24446
						MRE	0.63996	0.78990	0.39947	0.65983	0.48891
					500	MSE	0.22575	0.70569	0.26599	0.13576	0.06739
						ABB	0.41805	0.72807	0.42846	0.31163	0.18120
						MRE	0.55740	0.72506	0.28564	0.62325	0.36241

Table 8: Simulation results of the GLFRF distribution for several parametric values

λ	ϕ	γ	δ	λ	n		$\hat{\lambda}$	$\hat{\phi}$	$\hat{\gamma}$	$\hat{\delta}$	$\hat{\eta}$
					30	MSE	0.29157	0.61497	0.13891	0.25804	0.73206
						ABB	0.44763	0.68053	0.29978	0.35888	0.76176
						MRE	0.59684	0.68053	0.49964	0.25740	0.21765
					50	MSE	0.23196	0.54307	0.13228	0.22540	0.67023
						ABB	0.39572	0.61576	0.29437	0.32113	0.70076
						MRE	0.52763	0.61576	0.49061	0.23261	0.20022
0.75	1	0.6	1.2	3.5	200	MSE	0.16922	0.50956	0.09725	0.20717	0.48839
						ABB	0.33858	0.58531	0.25076	0.30629	0.55842
						MRE	0.45144	0.58531	0.41794	0.20191	0.15955
					500	MSE	0.11984	0.45463	0.06488	0.18033	0.40278
						ABB	0.28813	0.60908	0.20883	0.29041	0.48550
						MRE	0.38417	0.45908	0.34806	0.18200	0.13872

λ	ϕ	γ	δ	λ	n		$\hat{\lambda}$	$\hat{\phi}$	$\hat{\gamma}$	$\hat{\delta}$	$\hat{\eta}$
0.4	1	0.75	2.5	0.5	30	MSE	0.15548	0.87210	0.86808	0.68251	0.51478
						ABB	0.34464	0.91274	0.88104	0.95182	0.60266
						MRE	0.86159	0.91274	0.58736	0.38073	0.24532
					50	MSE	0.13837	0.81259	0.73259	0.64272	0.39390
						ABB	0.31860	0.87126	0.79576	0.91774	0.50678
						MRE	0.79651	0.87126	0.53051	0.35710	0.22136
					200	MSE	0.10209	0.56765	0.39464	0.55740	0.09785
						ABB	0.26566	0.68394	0.54094	0.84606	0.21479
						MRE	0.66416	0.68394	0.36063	0.31842	0.19958
					500	MSE	0.23503	0.87126	0.27030	0.49742	0.03795
						ABB	0.23503	0.58427	0.42513	0.75731	0.12396
						MRE	0.58757	0.58427	0.28342	0.29225	0.15792
0.4	1	1.5	0.5	0.5	30	MSE	0.14371	0.78486	0.87212	0.29788	0.50786
						ABB	0.33823	0.85310	0.97556	0.42582	0.61194
						MRE	0.84558	0.85310	0.65037	0.85163	0.95389
					50	MSE	0.14092	0.76253	0.81005	0.25590	0.35800
						ABB	0.32525	0.83315	0.87083	0.39394	0.48554
						MRE	0.81312	0.83315	0.58056	0.78788	0.89107
					200	MSE	0.12709	0.68781	0.47640	0.20609	0.10437
						ABB	0.29982	0.77064	0.60418	0.37112	0.22618
						MRE	0.74955	0.77064	0.40279	0.74225	0.45236
					500	MSE	0.09474	0.65322	0.33550	0.17395	0.03494

λ	φ	γ	δ	λ	n		$\hat{\lambda}$	$\hat{\phi}$	$\hat{\gamma}$	$\hat{\delta}$	$\hat{\eta}$
						ABB	0.26487	0.74067	0.48286	0.35618	0.12375
						MRE	0.66217	0.74067	0.32191	0.71236	0.24750

Table 9: Simulation results of the GLFRF distribution for several parametric values

λ	φ	γ	δ	η	n		$\hat{\lambda}$	$\hat{\phi}$	$\hat{\gamma}$	$\hat{\delta}$	$\hat{\eta}$
0.4	1	1.5	0.25	1.5	30	MSE	0.24010	0.84112	0.80190	0.01298	0.73961
						ABB	0.40657	0.88856	0.84509	0.09761	0.79980
						MRE	1.01642	0.88856	0.56339	0.39044	0.53320
					50	MSE	0.23213	0.79426	0.72241	0.01213	0.67461
						ABB	0.39390	0.85538	0.78829	0.09285	0.74848
						MRE	0.98476	0.85538	0.52553	0.37140	0.49899
					200	MSE	0.14011	0.71899	0.47685	0.00946	0.37535
						ABB	0.30464	0.79761	0.59768	0.07951	0.49432
						MRE	0.76160	0.79761	0.39846	0.31804	0.32955
					500	MSE	0.09767	0.69068	0.34682	0.00826	0.20278
						ABB	0.26150	0.77057	0.49051	0.07552	0.33056
						MRE	0.65374	0.77057	0.32701	0.30209	0.22037
0.4	0.5	0.6	0.25	0.5	30	MSE	0.14998	0.32632	0.16797	0.08311	0.26215
						ABB	0.34988	0.43551	0.35821	0.22400	0.42626
						MRE	0.87471	0.87103	0.59702	0.89599	0.85252
					50	MSE	0.14509	0.22990	0.15144	0.06666	0.17296
						ABB	0.33568	0.41700	0.32229	0.20290	0.33257
						MRE	0.83920	0.77399	0.53715	0.81161	0.66515

λ	ϕ	γ	δ	η	n		$\hat{\lambda}$	$\hat{\phi}$	$\hat{\gamma}$	$\hat{\delta}$	$\hat{\eta}$
					200	MSE	0.10324	0.15430	0.07771	0.06256	0.07180
						ABB	0.28272	0.35162	0.21975	0.20663	0.19906
						MRE	0.70681	0.65325	0.36626	0.75653	0.39811
					500	MSE	0.24154	0.77399	0.04465	0.06174	0.04705
						ABB	0.24154	0.25946	0.17028	0.21663	0.15726
						MRE	0.60385	0.51891	0.28380	0.66654	0.31452
0.4	1	0.6	0.25	0.5	30	MSE	0.16965	0.67600	0.18025	0.07163	0.29395
						ABB	0.36433	0.73750	0.36629	0.22174	0.44891
						MRE	0.91084	0.73750	0.61049	0.88696	0.89782
					50	MSE	0.14846	0.66143	0.15531	0.05567	0.18196
						ABB	0.34080	0.72607	0.32825	0.20306	0.34115
						MRE	0.85200	0.72607	0.54709	0.81223	0.68231
					200	MSE	0.11023	0.61150	0.10196	0.04664	0.09221
						ABB	0.29173	0.70260	0.25327	0.18180	0.21911
						MRE	0.72932	0.70126	0.42212	0.72718	0.43822
					500	MSE	0.07930	0.49251	0.07415	0.04100	0.04394
						ABB	0.24919	0.56603	0.21825	0.17155	0.14813
						MRE	0.62298	0.56603	0.36376	0.68618	0.29627

KF: $f(x) = ab\beta\alpha^{\beta} x^{-(\beta+1)} \exp\left[-a\left(\frac{\alpha}{x}\right)^{\beta}\right]\left\{1 - \exp\left[-a\left(\frac{\alpha}{x}\right)^{\beta}\right]\right\}^{b-1}$;

KMOF: $f(x) = \alpha\beta ab\delta^{\beta}x^{-\beta-1}\exp\left[-a\left(\frac{\delta}{x}\right)^{\beta}\right]\left\{\alpha + (1-\alpha)\exp\left[-\left(\frac{\delta}{x}\right)^{\beta}\right]\right\}^{-a-1}$

$$\times \left\{ 1 - \exp\left[-a\left(\frac{\delta}{x}\right)^{\beta}\right]\left\{\alpha + (1-\alpha)\exp\left[-\left(\frac{\delta}{x}\right)^{\beta}\right]\right\}^{-a} \right\}^{b-1} ;$$

BF: $f(x) = \frac{\beta \alpha^{\beta}}{B(a,b)} \, x^{-(\beta+1)} \exp\left[-a\left(\frac{\alpha}{x}\right)^{\beta}\right] \left\{1 - \exp\left[-\left(\frac{\alpha}{x}\right)^{\beta}\right]\right\}^{b-1} ;$

EF: $f(x) = \theta \beta \alpha^{\beta} \, x^{-(\beta+1)} \exp\left[-\left(\frac{\alpha}{x}\right)^{\beta}\right] \left\{1 - \exp\left[-\left(\frac{\alpha}{x}\right)^{\beta}\right]\right\}^{\theta-1} ;$

GEF: $f(x) = \frac{a \beta \alpha^{\beta}}{\Gamma(b)} \, x^{-(\beta+1)} \exp\left[-\left(\frac{\alpha}{x}\right)^{\beta}\right] \left\{1 - \exp\left[-\left(\frac{\alpha}{x}\right)^{\beta}\right]\right\}^{a-1}$

$$\times \left\{ -\log\left\{1 - \exp\left[-\left(\frac{\alpha}{x}\right)^{\beta}\right]\right\}^{a} \right\}^{b-1} ;$$

TF: $f(x) = \beta \alpha^{\beta} x^{-\beta-1} \exp\left[-\left(\frac{\alpha}{x}\right)^{\beta}\right] \left\{\lambda + 1 - 2\lambda \exp\left[-\left(\frac{\alpha}{x}\right)^{\beta}\right]\right\}.$

The parameters of all above models are positive real numbers except for the TF distribution for which $|\lambda| \leq 1$.

The competing distributions are compared using some measures such as the $-2\hat{\ell}$, Akaike information criterion (AIC), consistent AIC (CAIC), Bayesian information criterion (BIC) and Hannan-Quinn information criterion (HQIC), where $\hat{\ell}$ is the maximized log-likelihood. Furthermore, the Cramér-von Mises (W^*) and Anderson-Darling (A^*) statistics are als calculated.

These measures are defined by the following formula:

$AIC = -2\hat{\ell} + 2\mathcal{P},$

$CAIC = -2\,\hat{\ell} + \dfrac{2\,\mathcal{P}\,n}{(n - \mathcal{P} - 1)},$

$BIC = -2\,\hat{\ell} + \mathcal{P}\log(n),$

$HQIC = -2\,\hat{\ell} + 2\,\mathcal{P}\log[\log(n)],$

$W^* = \left(1 + \dfrac{1}{2\,n}\right)\left\{\sum_{k=1}^{n}\left(z_k - \dfrac{2k-1}{2\,n}\right)^2 + \dfrac{1}{12\,n}\right\}$

and

$$A^* = \left(1 + \frac{3}{4\,n} + \frac{9}{4\,n^2}\right)\left\{n + \sum_{k=1}^{n} \frac{(2\,k-1)}{n} \log[z_k\,(1 - z_{n-k+1})]\right\},$$

where $\hat{\ell}$ is the maximized log-likelihood, $\mathcal{P}$ is the number of estimated model parameters and n is the sample size, and $z_k = \text{CDF}(y_k)$, where y_k (for $k = 1, 2, \ldots, n$) are the ordered observations.

Tables 10 and 12 list the values of different goodness-of-fit measures, for the two data sets, to compare the GLFRF model with the other competing distributions. The values in these tables show that the GLFRF distribution gives the lowest values for all measure among all competing models. Tables 11 and 13 provide the MLEs for all compared models along with their standard errors (SEs) of these estimates.

Table 10: Goodness-of-fit smeasures for glass fibres data

Model	-2ℓ	$CAIC$	AIC	BIC	$HQIC$	W^*	A^*
GLFRF	29.011	40.064	39.011	49.727	43.226	0.22045	1.20310
KF	39.915	48.605	47.915	56.487	51.287	0.42986	2.35117
KMOF	32.682	43.735	42.682	53.398	46.897	0.29216	1.59683
BF	34.817	43.507	42.817	51.390	46.189	0.33337	1.81855
EF	39.201	45.608	45.201	51.631	47.730	0.41685	2.27979
GEF	39.418	48.108	47.418	55.991	50.790	0.41990	2.28765
TF	86.303	92.710	92.303	98.733	94.832	1.12662	6.01100
F	93.707	97.907	97.707	101.993	99.392	1.22546	6.48658

Table 11: MLEs and the corresponding SEs (in parentheses) for glass fibres data

Model	Estimates				
GLFRF	2.8189	1263.0888	0.4135	4.2941	1.3758
$(\lambda, \phi, \gamma, \delta, \eta)$	(4.1933)	(1546.1034)	(0.1949)	(1.2537)	(0.3456)
KF	13.9964	0.7561	1.2803	723.4195	
(α, β, a, b)	(189.9810)	(0.1115)	(13.1471)	(666.9131)	
KMOF	197.4702	2.4941	0.4391	2.4760	215.4915
$(\alpha, \beta, \delta, a, b)$	(254.9519)	(1.0800)	(0.2851)	(1.2496)	(398.0855)
BF	13.5591	1.0316	0.3941	2326.7155	
(α, β, a, b)	(7.1795)	(0.2566)	(0.1779)	(2492.018)	
EF	24.2254	0.7177	1110.7440		
(α, β, θ)	(13.8993)	(0.1073)	(1096.297)		
GEF	6.7186	1.3120	207.6693	0.3976	
(α, β, a, b)	(0.4521)	(0.0994)	(147.7114)	(0.1405)	

Model	Estimates				
TF (α, β, λ)	1.0937 (0.0560)	3.2217 (0.2564)	-0.7745 (0.1560)		
F (δ, η)	1.2643 (0.0588)	2.8876 (0.2344)			

The probability-probability (PP) plots of the GLFRF distribution and other distributions, are displayed in Figures 3 and 5, for the two data. Figures 4 and 5 show the estimated CDFs for both data sets. These plots support the numerical results in Tables 10 and 12. In concusion, the GLFRF distribution is recommended to model the two studied data sets.
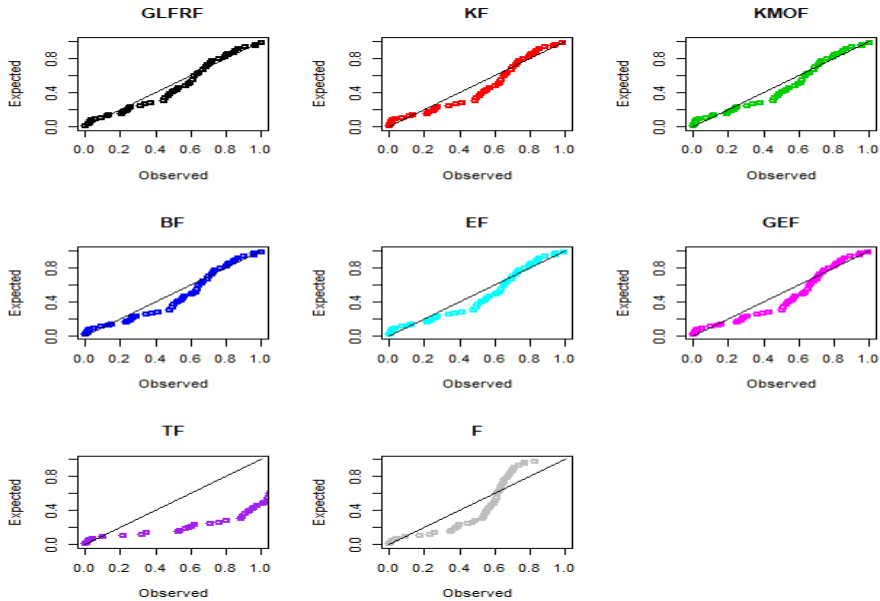
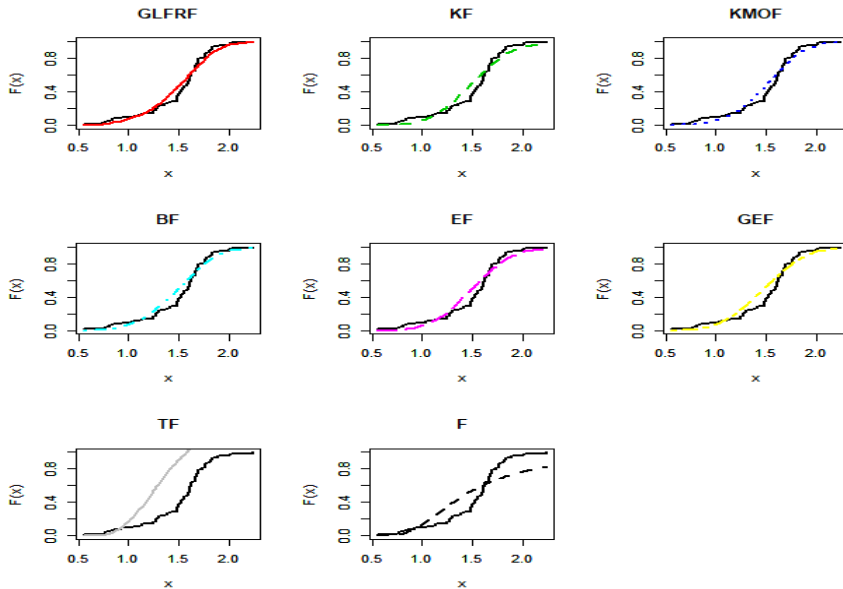Figure 3: The PP plots of competing distributions for glass fibres data

Figure 4: Fitted CDFs on empirical CDF for glass fibres data

Table 12: Goodness-of-fit smeasures for Wheaton river data

Model	-2ℓ	CAIC	AIC	BIC	HQIC	W^*	A^*
GLFRF	498.023	508.932	508.023	519.406	512.555	0.05919	0.37091
KF	506.005	514.602	514.005	523.112	517.630	0.17337	0.97379
KMOF	502.154	513.063	512.154	523.537	516.686	0.13817	0.76472
BF	514.765	523.362	522.765	531.872	526.39	0.28585	1.61240
EF	512.243	518.596	518.243	525.073	520.962	0.24225	1.37968
GEF	514.651	523.248	522.651	531.758	526.277	0.28449	1.60447
TF	529.984	536.337	535.984	542.814	538.703	0.41857	2.42652
F	534.038	538.212	538.038	542.591	539.851	0.48147	2.80181

Table 13: MLEs and the corresponding SEs (in parentheses) for Wheaton river data

Model	Estimates				
GLFRF	0.05222	0.01088	0.52208	1.34291	0.85289
$(\lambda, \phi, \gamma, \delta, \eta)$	(0.05330)	(0.02583)	(0.24290)	(1.19238)	(0.17727)
KF	6.3401	0.1332	6.6065	478.3001	
(α, β, a, b)	(0.011)	(0.00017)	(0.011)	(0.132)	
KMOF	89263.64	0.6814	0.2556	1.2323	54816.88
$(\alpha, \beta, \delta, a, b)$	(224.9697)	(0.0619)	(0.4076)	(0.1503)	(15004.53)
BF	38.2262	0.1356	11.712	30.3168	
(α, β, a, b)	(118.541)	(0.082)	(20.38)	(34.144)	

Model	Estimates			
EF (α,β,θ)	391.9297 (398.185)	0.2677 (0.033)	14.4425 (6.62)	
GEF (α,β,a,b)	40.4813 (129.175)	0.1345 (0.081)	35.7391 (42.978)	11.7358 (20.235)
TF (α,β,λ)	1.5083 (0.4374)	0.7107 (0.0589)	-0.7289 (0.2338)	
F (δ,η)	2.879 (0.553)	0.6521 (0.054)		
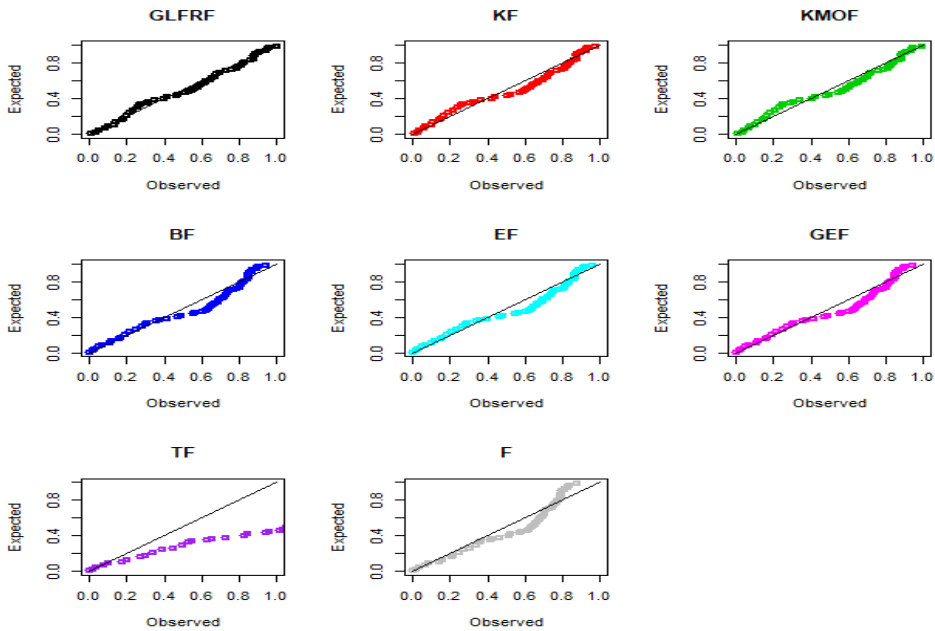
Figure 5: PP plots of compared distributions for Wheaton river data
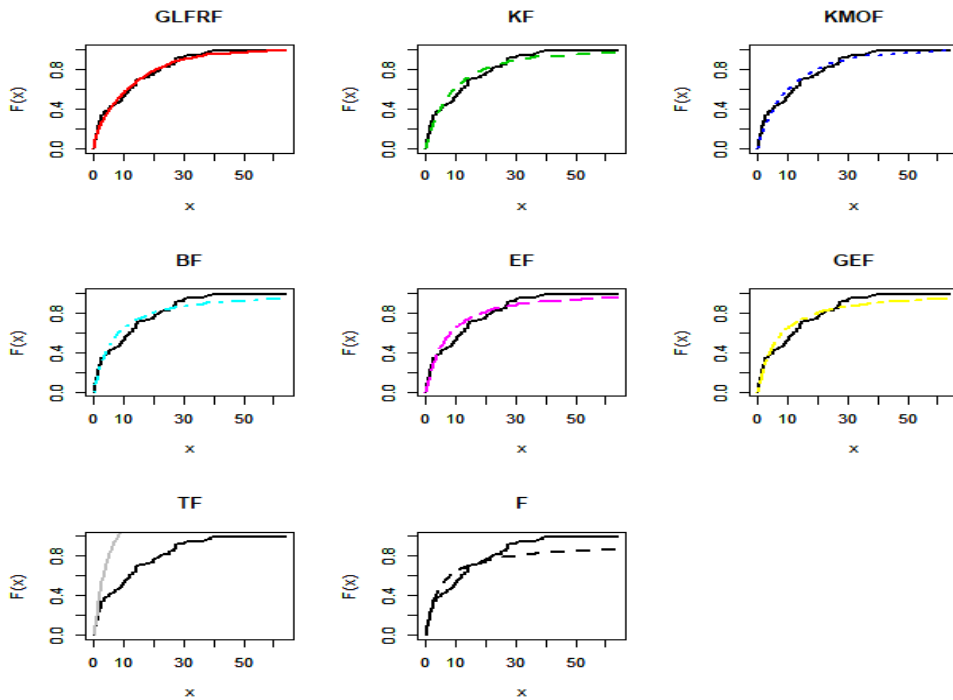
Figure 6: Fitted CDFs on empirical CDF for Wheaton river data

9. Conclusions

In this paper, we propose a new flexible extension of the Fréchet distribution called the generalized linear failure rate Fréchet (GLFRF) distribution. The important feature of the GLFRF distribution its hazard rate flexibility. Its hazard rate can be bathtub, modified bathtub, increasing, decreasing, and unimodal shapes. The quantile and generating functions, moments, order statistics, moments of residual and reversed residual lifes of the GLFRF distribution are provided in explicit expressions. The GLFRF parameters are estimated via the maximum likelihood. The GLFRF distribution is fitted to two real-life data and compared to other competing Fréchet distributions. It fits very well than these models.

References

Abouelmagd, T. H. M., Hamed, M. S., Afify, A. Z., Al-Mofleh, H. and Iqbal, Z. (2018). *The Burr X Fréchet distribution with its properties and applications. J. Appl. Prob. Stat.,* 13, 23–51.

Afify, A. Z., Hamedani, G. G., Ghosh, I. and Mead, M. E. (2015). The transmuted Marshall-Olkin Fréchet distribution: properties and applications. *International Journal of Statistics and Probability,* 4, 132-184.

Afify, A. Z., Marzouk, W., Al-Mofleh, H., Ahmed, A. H. N. and Abdel-Fatah, N. A., (2022). The extended failure rate family: properties and applications in the engineering and insurance fields. Pak. J. Statist, 38, 165-196.

Afify, A. Z., Shawky, A. and Nassar, M. (2021). A new inverse Weibull distribution: properties, classical and Bayesian estimation with applications. Kuwait J. Sci., 48, 1–10.

Afify, A. Z., Yousof, H. M., Cordeiro, G. M., Nofal, Z. M. and Ahmed, A. N. (2016a). The Kumaraswamy Marshall-Olkin Fréchet distribution with applications. *Journal of ISOSS*, 2, 41-58.

Afify, A. Z., Yousof, H. M., Cordeiro, G. M. Ortega, E. M. M. and Nofal, Z. M. (2016b) The Weibull Fréchet distribution and its applications. *Journal of Applied Statistics*, 43, 2608-2626.

Al Sobhi, M. M. (2021). The modified Kies–Frechet distribution: properties, inference and application. *AIMS Math*., 6, 4691–4714.

Barreto-Souza, W. M., Cordeiro, G. M. and Simas, A. B. (2011). Some results for beta Fréchet distribution. *Communications in Statistics - Theory and Methods,* 40, 798-811.

Dias, C. R., Cordeiro, G. M., Alizadeh, M., Marinho, P. R. D. and Coêlho, H. F. C. (2016). Exponentiated Marshall-Olkin family of distributions. *Journal of Statistical Distributions and Applications,* 3(1), p.15.

Elbatal, I. Asha, G. and Raja, V. (2014). Transmuted exponentiated Fréchet distribution: properties and applications. *Journal of Statistics Applications an Probability*, 3, 379-394.

Feigl, P. and Zelen, M. (1965). Estimation of Exponential Probabilities with Concomitant Information. *Biometrics,* 21, 826-838.

Fréchet, M. (1924). Sur la Loi des Erreurs d'Observation. Bulletin de la Soci et e *Math ematique de Moscou*, 33, 5-8.

Harlow, D. G. (2002). Applications of the Fréchet distribution function. International *Journal of Materials and Product Technology*, 17, 482-495.

Hussein, E.A., Aljohani, H.M. and Afify, A.Z. (2022). The extended Weibull–Fréchet distribution: properties, inference, and applications in medicine and engineering. *AIMS Mathematics*, 7, 225-246.

Krishna, E., Jose, K. K., Alice, T. and Ristic, M. M. (2013). The Marshall-Olkin Fréchet distribution. *Communications in Statistics-Theory and Methods,* 42, 4091-4107.

Kotz, S. and Nadarajah, S. (2000). *Extreme value distributions: theory and*

applications. Imperial College Press, London.

Lai, C. D. and Xie, M. (2006). *Stochastic ageing and dependence for reliability*. Springer, New York.

Mahmoud, M. R. and Mandouh, R. M. (2013). On the transmuted Fréchet distribution. *Journal of Applied Sciences Research*, 9, 5553-5561.

Mansour, M. M., Abd Elrazik, E. M., Altun, E., Afify, A. Z. and Iqbal, Z. (2018). A new three-parameter Fréchet distribution: properties and applications, *Pak. J. Stat.*, 34 (2018), 441–458.

Mead, M. E. and Abd-Eltawab A. R. (2014). A note on Kumaraswamy Fréchet distribution. *Australian Journal of Basic and Applied Sciences*, 8, 294-300.

Mead, M. E., Afify, A. Z., Hamedani, G. G. and Ghosh, I. (2017). The beta exponential Fréchet distribution with applications. *Austrian Journal of Statistics,* 46, 41-63.

Nadarajah, S. and Gupta, A. K. (2004). The beta Fréchet distribution. *Far East Journal of Theoretical Statistics*, 14, 15-24.

Nadarajah, S. and Kotz, S. (2003). The exponentiated Fréchet distribution. *Interstat Electronic Journal*, 1-7.

Resnick, S. I. (2013). *Extreme values, regular variation and point processes.* Springer, New York.

Silva, R. V. D., de Andrade, T. A., Maciel, D., Campos, R. P., and Cordeiro, G. M. (2013). A new lifetime model: the gamma extended Fréchet distribution. *Journal of Statistical Theory and Applications,* 12, 39-54.

Tablada, C. J. and Cordeiro, G. M. (2017). The modified Fréchet distribution and its properties. *Communications in Statistics-Theory and Methods, forthcoming.*

Zaharim, A., Najid, S. K., Razali, A. M. and Sopian, K. (2009). Analysing Malaysian wind speed data using statistical distribution. In Proceedings of the 4th IASME/WSEAS *International conference on energy and environment*, Cambridge, UK.